# The proteome of Toll-like receptor 3–stimulated human immortalized fibroblasts: Implications for susceptibility to herpes simplex virus encephalitis

**Rebeca Pérez de Diego, PhD,[a,b,c,d] Claire Mulvey, PhD,[e] Mark Crawford, BSc,[e] Matthew W. B. Trotter, PhD,[f] Lazaro Lorenzo, BSc,[a,b,c] Vanessa Sancho-Shimizu, PhD,[a,b,c] Laurent Abel, MD, PhD,[a,b,c] Shen-Ying Zhang, MD, PhD,[a,b,c] Jean-Laurent Casanova, MD, PhD,[a,b,c,g,h] and Jasminka Godovac-Zimmermann, PhD[e]** *Paris, France, New York, NY, Madrid, Spain, London and Cambridge, United Kingdom, and Riyadh, Saudi Arabia*

**Background: Inborn errors in Toll-like receptor 3 (TLR3)-IFN type I and III pathways have been implicated in susceptibility to herpes simplex virus encephalitis (HSE) in children, but most patients studied do not carry mutations in any of the genes presently associated with HSE susceptibility. Moreover, many patients do not display any TLR3-IFN-related fibroblastic phenotype.**

**Objective: To study other signaling pathways downstream of TLR3 and/or other independent pathways that may contribute to HSE susceptibility.**

**Methods: We used the stable isotope labeling of amino acids in cell culture proteomics methodology to measure changes in the human immortalized fibroblast proteome after TLR3 activation.**

**Results: Cells from healthy controls were compared with cells from a patient with a known genetic etiology of HSE (UNC-93B$^{-/-}$) and also to cells from an HSE patient with an unknown gene defect. Consistent with known variation in susceptibility of individuals to viral infections, substantial variation in the response level of different healthy controls was observed, but common functional networks could be identified, including upregulation of superoxide dismutase 2. The 2 patients with HSE studied show clear differences in functional response networks when compared with healthy controls and also when compared with each other.**

**Conclusions: The present study delineates a number of novel proteins, TLR3-related pathways, and cellular phenotypes that may help elucidate the genetic basis of childhood HSE. Furthermore, our results reveal superoxide dismutase 2 as a potential therapeutic target for amelioration of the neurologic sequelae caused by HSE. (J Allergy Clin Immunol 2013;131:1157-66.)**

***Key words:*** *Herpes simplex virus encephalitis (HSE), SILAC, proteomics, mass spectrometry, fibroblast, herpes simplex virus 1 (HSV-1), TLR3, IFN*

Herpes simplex virus encephalitis (HSE) is a devastating infection of the central nervous system (CNS).[1] It is the most common form of sporadic viral encephalitis in Western countries, where it is estimated to occur in approximately 1 in 250,000 individuals per year. It peaks in childhood between the ages of 3 months and 6 years during primary infection with herpes simplex virus 1 (HSV-1), which reaches the CNS via a neurotropic route involving the trigeminal and olfactory nerves.[2,3] Treatment with acyclovir decreases the mortality rate in affected children, but significant neurologic impairment is observed in most survivors, young children in particular. HSV-1 is widespread and typically innocuous in human populations. Childhood HSE has not been associable with known immunodeficiencies, and its pathogenesis remained elusive until we identified the first 3 genetic etiologies of this condition.[4,5] Autosomal-recessive UNC-93B deficiency abolishes Toll-like receptor 3 (TLR3), TLR7, TLR8, and TLR9 signaling,[6] whereas autosomal-dominant TLR3 deficiency specifically affects TLR3 signaling.[7] Recently, an autosomal-dominant deficiency in TNF receptor–associated factor 3 (TRAF3), an adaptor molecule implicated in the TLR3 pathway, Toll/IL1R domain-containing adaptor inducing IFN-β (TRIF) and TANK-binding kinase (TBK1)–deficient patients has been described.[8-10] These studies suggested that childhood HSE may result from impaired IFN-α/β and IFN-λ production in response to the stimulation of TLR3 by double-stranded RNA intermediates of HSV-1 in the CNS. However, only a small fraction of children with HSE carry mutations in *UNC93B1*, *TLR3*, *TRAF3*, *TRIF*, or *TBK1*. The study of proteins implicated in the TLR3-IFN pathway for patients with HSE enrolled in our laboratory

From [a]Laboratory of Human Genetics of Infectious Diseases, Necker Branch, Necker Medical School, Paris; [b]University Paris Descartes, Paris; [c]St Giles Laboratory of Human Genetics of Infectious Diseases, Rockefeller Branch, The Rockefeller University, New York; [d]Immunology Unit, IdiPAZ Institute for Health Research, La Paz University Hospital, Madrid; [e]the Division of Medicine, University College London, London; [f]The Anne McLaren Laboratory for Regenerative Medicine and Department of Surgery, University of Cambridge, Cambridge; [g]the Department of Pediatrics, Prince Naif Center for Immunology Research, College of Medicine, King Saud University, Riyadh; and [h]the Pediatric Hematology-Immunology Unit, Necker Hospital, Paris.

This study was supported by the AXA Research Fund, Groupement d'Intérêt Scientifique Maladies Rares, Action Concertée Incitative de Microbiologie, the March of Dimes, Agence Nationale pour la Recherche, the Eppley Foundation, the National Institute of Allergy and Infectious Diseases (grant no. R01AI088364), the Thrasher Research Fund, the Jeffrey Modell Foundation, Talecris Biotherapeutics, the St Giles Foundation, the National Center for Advancing Translational Sciences (NCATS) of the National Institutes of Health (NIH) (grant no. 8UL1TR000043), and the Rockefeller University.

Disclosure of potential conflict of interest: R. P. de Diego is supported by a European Union FP6 grant. J.-L. Casanova was an international scholar of the Howard Hughes Medical Institute until 2008. J. Godovac-Zimmermann was supported by a Wellcome Trust Grant. Since initial involvement in the work, M. W. B. Trotter has become an employee of Celgene Research SLU, part of Celgene Corporation, and declares no conflicts of interest. The rest of the authors declare that they have no relevant conflicts of interest.

Received for publication July 22, 2012; revised December 13, 2012; accepted for publication January 10, 2013.

Available online February 21, 2013.

Corresponding author: Rebeca Perez de Diego, PhD, Immunology Unit, IdiPAZ Institute for Health Research, La Paz University Hospital, 261 P° Castellana, Madrid 28046, Spain. E-mail: rebeca.perez@idipaz.es or perezdediegor@gmail.com.

0091-6749/$36.00



http://dx.doi.org/10.1016/j.jaci.2013.01.008

*Abbreviations used*
CNS: Central nervous system
H: Heavy medium
HSE: Herpes simplex virus encephalitis
HSV-1: Herpes simplex virus 1
1ICAM-1: Intercellular adhesion molecule-1
L: Light medium
MS: Mass spectrometry
poly(I:C): Polyinosinepolycytidylic acid
PPIF: Peptidyl-propyl cis-trans isomerise mitochondrial
SILAC: Stable isotope labeling of amino acids in cell culture
SOD2: Superoxide dismutase 2
TLR3: Toll-like receptor 3

(226 patients) has revealed that only a small proportion of patients bear a genetic defect in these proteins. A larger proportion of patients display an impaired production of IFN type I and III on TLR3 stimulation of their fibroblasts. Other patients do not show the fibroblastic phenotype associated with impaired IFN production; in these patients, the gene defect may affect other pathway(s) that are normally activated in fibroblasts after TLR3 stimulation. In the present study, as an approach to define new candidate genes for HSE, we have used proteomics methods to characterize TLR3-dependent pathways in fibroblasts that might be correlated with HSV-1 infection in the CNS.

## METHODS

### Subjects and patient P case report

The experimental protocol was approved by the Ethical Committee of Necker-Enfants Malades Hospital (Paris, France), and written informed consent was obtained for this study. P is a French boy of nonconsanguineous descent with no family history of encephalitis. At the age of 8 years, he suffered fever, convulsions, and hemiparesis and he was diagnosed with HSE.

### Cell purification

Primary human fibroblasts were obtained from biopsies of an UNC-93B–deficient patient,[6] 3 healthy controls, and 1 HSE patient with unknown gene defect. They were then transformed with an SV-40 vector, as previously described,[11] to create immortalized fibroblast cell lines: SV40 fibroblasts.

### Stable isotope labeling with amino acids in cell culture labeling of human SV40 fibroblasts

Cells were grown for 6 rounds of cell division in Dulbecco modified Eagle medium containing 13C6, 15N4 L-arginine, and 13C6 L-lysine (Invitrogen, Carlsbad, Calif) (heavy medium [H]) supplemented with 10% dialyzed FCS (Invitrogen) to ensure that all the cellular proteins were labeled to saturation. The stable isotope labeling of amino acids in cell culture (SILAC) technique relies on the intrinsic metabolic machinery of the cell to incorporate "heavy" amino acids into all newly synthesized proteins. Immortalized fibroblast cell lines were used to achieve the full SILAC incorporation without detrimentally affecting the characteristics of the cell line. Our previous work has demonstrated that SV40-immortalized fibroblasts can successfully be used to study TLR3 signaling.[7-9]

Labeled cells were activated in 24-well plates, at a density of $10^5$ cells/well, with 25 μg/mL of polyinosinepolycytidylic acid (poly[I:C]), a TLR3 agonist (InvivoGen, San Diego, Calif), for 24 hours. Unlabeled cells were grown in parallel in medium containing normal amino acids (light medium [L]) and were not stimulated. The SILAC labels were shown to be fully incorporated before the experiment was conducted (data not shown).

### Protein separation and in-gel enzymatic digestion

Equal amounts of protein from unlabeled "light" (nonstimulated) and labeled "heavy" (stimulated) cells were mixed and subsequently separated by using SDS-PAGE (BioRad Laboratories, Hercules, Calif). Proteins were visualized by silver staining (Sigma, St Louis, Mo), and the gel lane was divided into approximately 34 equally sized pieces that were excised from the gel and destained (30 mmol/L $K_3Fe(CN)_6$; 100 mmol/L $Na_2S_2O_3$) prior to further processing. Gel processing was conducted with a Progest Investigator Instrument (DigiLab, Genomics Solutions, Cambridgeshire, United Kingdom) for reduction and alkylation according to established protocols.[12] Briefly, the gel pieces were washed with 3 cycles of 25 mmol/L $NH_4HCO_3$ (pH 8.0) and acetonitrile. Finally, gel plugs were rehydrated in 20 μg/mL of sequencing grade modified trypsin (Promega, Hampshire, United Kingdom) and incubated overnight at 37°C. Tryptic peptides were eluted, vacuum-dried, and resuspended in 0.1% formic acid.

XCalibur raw files were processed by using Quant.exe and Identify.exe of the MaxQuant suite (version 1.0.13.13), in combination with the Mascot search engine (version 2.2; Matrix Science, London, United Kingdom), and searched against a concatenated International Protein Index human protein database (version 3.54; containing 75,710 entries, including 262 commonly observed contaminants such as porcine trypsin and some human keratins). All proteins were filtered according to a false discovery rate of 1% applied at both peptide and protein levels. Proteins were automatically quantified in the MaxQuant software. In the final results files, all protein groups with a normalized ratio significance B score of .05 or less and a normalized ratio of more than 1.5 were accepted for downstream analysis. Experiments were done in duplicate, and all proteins discussed in the text were significant in both replicates for each sample. For details of mass spectrometry (MS) analysis, protein inference and quantification, analysis of sample correlations, and global functional analysis of protein networks, see Additional methods in this article's Online Repository available at www.jacionline.org.

### Transient transfections

SV40 fibroblasts were transfected with 2 μg of pBI-EGFP-MnSOD (superoxide dismutase 2 [SOD2]) or pTRE-Tight-BI-AcGFP1 (Clontech, Palo Alto, Calif) as mock vector, in the presence of the FuGENE HD Transfection Reagent (Roche Applied Science, Indianapolis, Ind), according to manufacturer's instructions. Twenty-four hours posttransfection, SV40 fibroblasts were activated by incubation with 25 μg/mL of poly(I:C) (InvivoGen) for 24 hours. pTRE-Tight-BI-AcGFP1 was used as mock vector (pBI-EGFP has been replaced by AcGFP; it has 94% identical amino acid sequence and same biophysical properties).

### Western blot

Total cell extracts were prepared from SV40 fibroblasts, both transfected and not transfected. Equal amounts of protein from each sample were separated by using SDS-PAGE and blotted onto iBlot Gel Transfer Stacks (Invitrogen). Membranes were probed with anti–intercellular adhesion molecule-1 (ICAM-1) rabbit monoclonal (Lifespan Biosciences, Seattle, Wash), anti-SOD2 and ITGA2 monoclonals and anti-ITGA5 and peptidyl-propyl cis-trans isomerise mitochondrial (PPIF) polyclonals (Abcam, Cambridge, Mass), anti-ANXA5/7 monoclonals (SantaCruz Biotechnology, Inc, Santa Cruz, Calif), followed by a secondary antimouse or antirabbit IgG (GE Healthcare, Buckinghamshire, United Kingdom). Membranes were stripped and reprobed with anti-glyceraldehyde-3-phosphate dehydrogenase (SantaCruz) to control for protein loading. Antibody binding was detected by using enhanced chemiluminescence (Amersham-Pharmacia-Biotech, Buckinghamshire, United Kingdom).

### Apoptosis analysis

Levels of SV40-fibroblast apoptosis after poly(I:C) stimulation were assessed by measures of caspase-3 and caspase-7 activity. Cells were plated, in triplicate, in Microtest 96-well Assay Plate, Optilux Black/Clear Bottom (Falcon; Becton Dickinson, Franklin Lakes, NJ) ($1 \times 10^4$ cells/well), in Dulbecco modified Eagle medium supplemented with 2% FCS; some cells were

transfected with 150 ng/well of pBI-EGFP-MnSOD (SOD2) or pTRE-Tight-BI-AcGFP1 as mock vector. Twenty-four hours later, cells were treated with poly(I:C) (25 μg/mL) and incubated for 24 hours. Caspase-3 and caspase-7 activity was measured 48 hours posttransfection by using Caspase-Glo 3/7 Assay (Promega) as per manufacturer's instructions.

### IFN type I and III determination

SV40-fibroblast cell lines were activated in 24-well plates at a density of $10^5$ cells/well and stimulated with poly(I:C) at a concentration of 25 μg/mL for 24 hours. Cells were grown at 37°C under an atmosphere containing 5% $CO_2$. Cell supernatants were recovered, and an ELISA was performed for IFN-β (TFB; Fujirebio, Inc, Tokyo, Japan) according to manufacturer's instructions. The ELISA for IFN-λ was performed as previously described.[7]

## RESULTS

### Identification of proteins upregulated in human SV40 fibroblasts following TLR3 activation

Response to TLR3 activation was defined by altered levels of protein abundance in human SV40 fibroblasts when stimulated with poly(I:C) (used as TLR3 agonist[6-9]) and was measured by SILAC/MS[13-15] monitoring of heavy/light isotope labeling ratios for peptides from proteins of stimulated/unstimulated cells (Fig 1, *A*).

Three healthy samples (C1, C2, and C3) are positive controls that provide a measure of variability between individuals (Fig 1, *B*). Negative control, C2NS, is a healthy sample with strong TLR3 response, but for which neither cell population (light/heavy) was stimulated (Fig 1, *B*). The UNC-93B deficiency blocks TLR3, TLR7, TLR8, and TLR9 pathways, and so cells from the UNC-93B$^{-/-}$ patient (sample UNC-93B$^{-/-}$) should not respond to TLR3 agonists.[6] We used SV40 fibroblasts from a homozygous UNC-93B$^{-/-}$ patient rather than a patient with heterozygous TLR3 mutation because of the complete deficiency of TLR3 pathways observed in UNC-93B$^{-/-}$ cells.[6] Finally, we included cells from an HSE patient with unknown gene defect (P) (Fig 1, *B*), which produce detectable amounts of IFN type I after TLR3 stimulation (Fig 2).

All 6 biological samples were subjected to duplicate MS analysis,[16,17] and protein lists were obtained by combining both data sets prior to analysis of differential protein abundance (see Tables E1-E6 in this article's Online Repository available at www.jacionline.org). The MS data are summarized in Fig 1, *C*, and Fig E1 in this article's Online Repository available at www.jacionline.org illustrates the quality of the MS data for a single SILAC peptide pair detected in a key protein of our study.

Fig 1, *C*, shows the number of proteins found to be significantly upregulated (normalized H/L [SILAC] ratio ≥1.5 and significance B[17] <.05; see below) in the different cells following activation (except for C2NS) with poly(I:C). We have previously observed variability in response of healthy control fibroblasts on TLR3 stimulation, particularly in terms of cytokine and interferon production (Fig 2). To take this into account, we included sample C3, from a healthy donor with known weaker response to TLR3 stimulation compared with C1 and C2 (Fig 2). In line with expectation, this control showed a reduced number of upregulated proteins (19 with SILAC H/L ratios between 1.50-fold and 2.15-fold; Fig 1, *C*). Comparison of upregulated proteins between the control samples revealed variation in those proteins most strongly upregulated. This variability might arise from (a) the conservative condition that protein SILAC ratios were calculated from at least 3 separate H/L ratio measurements and/or (b) differences in the extent to which different proteins change in abundance in cells taken from different individuals. A qualitative test of cellular variability among healthy controls

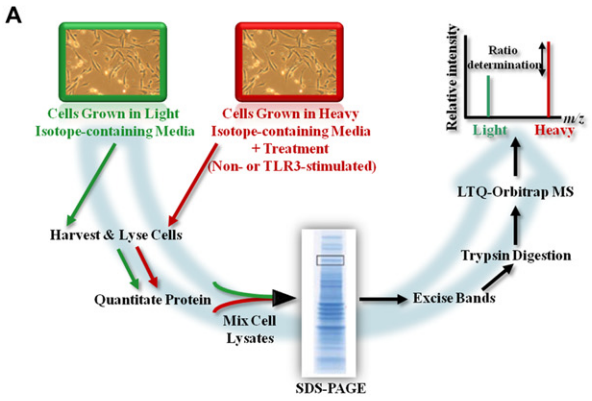


B

| | TLR3 stimulation with Poly(I:C) | TLR3 pathway in genetic terms | Final activation state for TLR3 |
|---|---|---|---|
| **C1, C2 and C3** | Yes | WT (healthy donor-1, 2 and 3 respectively) | **Activated** |
| **C2NS** | No | WT (healthy donor-2) | **Not activated due to non-stimulation** |
| **UNC-93B$^{-/-}$** | Yes | Blocked due to UNC93B deficiency (HSE patient) | **Not activated due to genetic defect** |
| **P** | Yes | Unknown gene defect (HSE patient) | **Unknown** |

C

| | C1 | C2 | C3 | C2NS | UNC-93B$^{-/-}$ | P |
|---|---|---|---|---|---|---|
| **SILAC experimental conditions** | L/NS + H/TLR3 | L/NS + H/TLR3 | L/NS + H/TLR3 | L/NS + H/NS | L/NS + H/TLR3 | L/NS + H/TLR3 |
| **Proteins identified*** | 2098 | 1790 | 1401 | 1665 | 1997 | 1834 |
| **Proteins quantified†** | 1614 | 1350 | 1023 | 1240 | 1640 | 1457 |
| **Significantly upregulated proteins‡** | 98 | 77 | 19 | 8 | 41 | 96 |
| **Number of MS full scans** | 387341 | 405545 | 408980 | 427364 | 411575 | 325169 |
| **Number of MS /MS scan events** | 128737 | 126579 | 168691 | 116717 | 128115 | 337310 |
| **Number of MS/MS identified** | 55184 | 54350 | 62702 | 49135 | 56786 | 80472 |
| **Peptide sequences identified** | 16335 | 13204 | 10044 | 11897 | 14256 | 12679 |
| **Number of SILAC pairs** | 43017 | 27730 | 34729 | 35473 | 43336 | 82196 |
| **Number of SILAC pairs sequenced** | 30353 | 22226 | 22662 | 24138 | 32952 | 44882 |
| **Number of SILAC pairs identified** | 16742 | 13784 | 12083 | 14315 | 19233 | 17377 |

**FIG 1. A,** Illustration of the SILAC workflow. **B,** Summary of samples used and TLR3 pathway state for the SILAC experiment. **C,** Overview of MS results obtained with MaxQuant software. *C1-3,* Healthy controls; *C2NS,* healthy control-2 nonstimulated; *H,* heavy medium; *L,* light medium; *NS,* nonstimulated cells; *P,* patient with unknown gene defect; *TLR3,* poly(I:C)-stimulated cells; *UNC-93B$^{-/-}$,* UNC-93B–deficient patient; *WT,* wild-type. *Protein groups identified with protein and peptide false discovery rate = 1%. †Protein abundance ratios calculated as median values using a minimum of 3 quantifiable razor peptides. ‡Protein ratios with significance B ≤.05 and SILAC ratios ≥1.5.

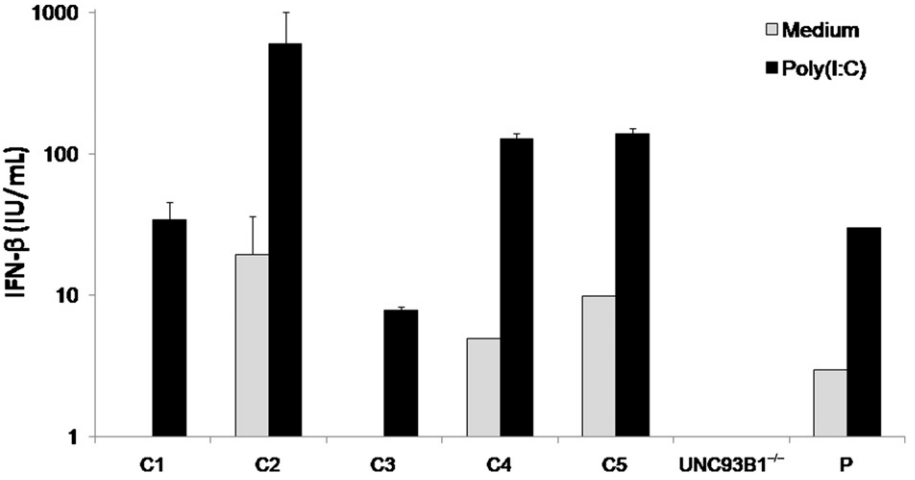


**FIG 2.** Production of IFN-β by SV40 fibroblasts after poly(I:C) stimulation for 24 hours as assessed by ELISA. Mean values ± SD were calculated from 3 independent experiments. *C1-C5*, Positive healthy controls; *UNC93B1*$^{-/-}$, UNC-93B–deficient patient.

displays biologically relevant positive correlation distinguishable from the negative control (C2NS) (see Additional results, Fig E2, Fig E3, and Table E7 in this article's Online Repository available at www.jacionline.org).

## Detection of functional networks

Given the observed variability in the detection and measurement of specific protein regulation across experiments, we sought common functional networks among the most strongly upregulated proteins to characterize response to TLR3 stimulation and identify disease-related differences by comparison. We used MetaCore version 6.3 (GeneGo, Inc) to investigate pathways and biological functions represented by differentially regulated proteins in all samples (see Additional results and Fig E2).

The analysis indicated that the most significant GeneGo process networks for C1/C2/C3 are similar and are implicated in immune responses, such as IFN-signaling and antigen presentation pathways (Table I), known to be implicated following TLR3 stimulation.[18,19] Similar analysis was performed for the nonstimulated C2NS control sample. The majority of proteins in the nonstimulated control C2NS show SILAC ratios of approximately 1 (Table E4), which represent "measurement noise." As may be expected, the 8 proteins designated as upregulated (H/L = 1.50-3.07-fold) did not associate with canonical pathways or process networks implicated in the immune response, and networks inferred from them were of limited statistical significance and scattered over diverse pathways and processes (Table II). The UNC-93B$^{-/-}$ sample did not associate with the immune-related networks identified above, further suggesting that the TLR3 pathway is completely abolished by this deficiency (Table II). UNC-93B$^{-/-}$ did, however, yield several upregulated proteins (Table E5), with SILAC ratios of 1.5 to 3.95-fold, which may represent attempts by these cells to compensate for the genetic defect. Canonical pathways associated with these proteins were largely metabolic (glycolysis, gluconeogenesis, fructose metabolism), however, and process networks inferred were particularly diverse (Table II).

The same analysis was also performed on the union of proteins upregulated in C1/C2/C3 (152 proteins, excluding 7 proteins in common with C2NS or UNC-93B$^{-/-}$ samples), strengthening the association between TLR3 stimulation and IFN-α/β signaling pathways (Table I; see Fig E4 in this article's Online Repository available at www.jacionline.org) and further suggesting a clear proteomic signature for the activation of these pathways on TLR3 stimulation.

The analysis of healthy controls also revealed other statistically significant proteins/pathways/processes (Table I) that do not appear in similar analysis of C2NS or UNC-93B$^{-/-}$ samples (Table II), and which have not been associated previously with TLR3 pathways. Such proteins included ICAM-1, integrins ITGA2 and ITGA5, and SOD2 (Table I). Furthermore, some proteins upregulated by TLR3 stimulation in healthy controls were not placed in pathways/networks by GeneGo but are associated with a role in HSV infection in the CNS by literature evidence. These proteins include several annexins and peptidyl-propyl cis-trans isomerise mitochondrial (PPIF) (Tables E1-E3), the majority of which were not identitied as differentially regulated by analysis of UNC-93B$^{-/-}$ (Fig 3, *A*). Table E8 in this article's Online Repository available at www.jacionline.org shows MS data for individual peptides assigned to these proteins and confirms the quality of their detection and assignment. The expression of these proteins was confirmed by western blot (see Fig E5 in this article's Online Repository available at www.jacionline.org), and they are considered further in the discussion.

Finally, although not the primary focus of our analysis, the union of proteins commonly downregulated on TLR3 stimulation in healthy controls C1/C2/C3 was subjected to similar pathway analysis. The results are summarized in Tables E1 to E3 and reflect strongest association with cytoskeleton remodeling and negative regulation of cell cycle, in accordance with the apoptosis induced on TLR3 stimulation and in agreement, for example, with the upregulation of annexins identified above.

## Proteomics of TLR3-stimulated fibroblasts reveals potential new treatments for HSE: SOD2 upregulation

SOD2 is highly upregulated in healthy patient samples C1, C2, and C3 after TLR3 stimulation but not in cells from a patient with

**TABLE I.** GeneGo pathway maps and process networks with their proteins associated

**Analysis of the individual data sets for C1–C3**

| C1 Sample | | C2 Sample | | C3 Sample | |
|---|---|---|---|---|---|
| **Name** | ***P* value** | **Name** | ***P* value** | **Name** | ***P* value** |
| **Ontology: Top GeneGo pathway maps** | | **Ontology: Top GeneGo pathway maps** | | **Ontology: Top GeneGo pathway maps** | |
| Immune response_Antigen presentation by MHC class I | .0004167 | Immune response_Antiviral actions of interferons | $5.215 \times 10^{-5}$ | Immune response_MIF-mediated glucocorticoid regulation | .02399 |
| Immune response_IFN alpha/beta signaling pathway | .007584 | Immune response_Antigen presentation by MHC class I | .0001645 | Immune response_IFN alpha/beta signaling pathway | .02615 |
| **Ontology: Top GeneGo process networks** | | **Ontology: Top GeneGo process networks** | | Immune response_IL-27 signaling pathway | .02615 |
| Inflammation_Interferon signaling | $4.681 \times 10^{-5}$ | Immune response_Antigen presentation | .0004169 | Immune response_Role of integrins in NK cells cytotoxicity | .04112 |
| Immune response_Phagosome in antigen presentation | .0006502 | Immune response_Phagosome in antigen presentation | .007849 | **Ontology: Top GeneGo process networks** | |
| Immune response_Antigen presentation | .00111 | Inflammation_Interferon signaling | .01796 | Inflammation_Interferon signaling | .01668 |
| | | | | Immune response_IL-5 signaling | .0779 |

**Enrichment analysis for the union of the C1–C3 data sets**

**Union C1, C2, and C3 Samples**

| Ontology: Top GeneGo pathway maps | | | Ontology: Top GeneGo process networks | | |
|---|---|---|---|---|---|
| **Name** | ***P* value** | **Proteins associated** | **Name** | ***P* value** | **Proteins associated** |
| Immune response_IFN alpha/beta signaling pathway | .007584 | ISG54, ISG15, PTP-1B | Inflammation_Interferon signaling | $4.68 \times 10^{-5}$ | TAP1, TAP2, ICAM-1, ISG15, ISG54, IFI56 |
| Immune response_MIF-mediated glucocorticoid regulation | .02399 | ICAM-1 | Immune response_Antigen presentation | .000417 | Tapasin, TAP1, TAP2, Calnexin, ICAM-1 |
| Immune response_IL-27 signaling pathway | .02615 | ICAM-1 | Inflammation_NK cell cytotoxicity | .04988 | Histone H1, ICAM-1, TfR1, MHC class 1 |

| Ontology: Top GeneGo pathway maps | | | Ontology: Top GeneGo process networks | | |
|---|---|---|---|---|---|
| **Name** | ***P* value** | **Proteins associated** | **Name** | ***P* value** | **Proteins associated** |
| Transcription_Role of AP-1 in regulation of cellular metabolism | .01016 | **ITGA2, ITGA5** | Blood coagulation | .000239 | TFPI-2, PLAU, **ITGA2, annexin V** |
| Chemotaxis_CCR4-induced leukocyte adhesion | .01171 | **ICAM-1**, Talin | Cell adhesion_Platelet-endothelium-leucocyte interactions | .000597 | **Integrins**, TFPI-2, PAI2, **ICAM-1**, PLAU, FGF2 |
| Apoptosis and survival_Endoplasmic reticulum stress response pathway | .01918 | ERP5, **SOD2** | Transcription_mRNA processing | .01563 | hnRNP F, SNRPA, HYPA, KHSRP, SAM68, DDX5, SF3B1, U2AF35 |
| Development_Cross-talk between VEGF and angiopoietin 1 signaling pathways | .0283 | **ICAM-1** | Cell adhesion_Attractive and repulsive receptors | .02102 | **ICAM-1, integrins**, cortactin |
| Chemotaxis_Inhibitory action of lipoxins on IL-8- and leukotriene B4-induced neutrophil migration | .0319 | **ICAM-1**, Talin | Proteolysis_Connective tissue degradation | .03509 | TFPI-2, IRAP, PAI2, PLAU |
| Inhibitory action of lipoxins on neutrophil migration | .03911 | **SOD2** | Cell adhesion_Cell-matrix interactions | .05649 | **Integrins** |
| Apoptosis and survival_Anti-apoptotic action of nuclear ESR1 and ESR2 | .04006 | **SOD2** | Cell adhesion_Integrin-mediated cell-matrix adhesion | .05697 | **Integrin**, Talin, CD82 |

Notes. Upper panels: Pathways/networks known to be implicated in TLR3-IFN signaling. Lower panels: New pathways/networks activated. Threshold: 1.5 (SILAC ratio), Significance B *P* value <.05. Sorting method is statistically significant. Boldface names are proteins with potential biological significance in HSE.

known genetic deficiency UNC-93B$^{-/-}$ and neither in unstimulated healthy control sample C2NS (Fig 3, *A*). SOD2 is an antioxidant enzyme strongly upregulated after TLR3 activation in macrophages, protecting these cells from oxidative stress during microbial infection.[20] SOD2 is increased after HSV-1 infection, and SOD2 levels in the CNS are associated with neuronal protection.[21,22] Other examples of the protective role of SOD2 have been shown in an animal model of complex I deficiency,[23] in which SOD2 gene transfer *in vivo* enhanced cellular resistance to reactive oxygen species and suppressed degeneration of the

**TABLE II.** GeneGo pathway maps and process networks after the analysis of the individual data sets for control nonstimulated (C2NS), UNC-93B–deficient patient cells (UNC-93B$^{-/-}$), and HSE patient cells with unknown gene defect (P)

| C2NS Sample | | UNC-93B$^{-/-}$ Sample | | P Sample | |
|---|---|---|---|---|---|
| **Name** | ***P* value** | **Name** | ***P* value** | **Name** | ***P* value** |
| **Ontology: Top GeneGo pathway maps** | | **Ontology: Top GeneGo pathway maps** | | **Ontology: Top GeneGo pathway maps** | |
| Cell adhesion_Cadherin-mediated cell adhesion | .00952 | Glycolysis and gluconeogenesis (short map) | $1.87 \times 10^{-9}$ | Apoptosis and survival_Granzyme A signaling | .00097 |
| Development_Slit-Robo signaling | .01098 | Glycolysis and gluconeogenesis p. 3/human version | $6.96 \times 10^{-5}$ | Transcription_P53 signaling pathway | .0021 |
| Neurophysiologic process_EphB receptors in dendritic spine morphogenesis and synaptogenesis | .0128 | Glycolysis and gluconeogenesis p. 3 | $6.96 \times 10^{-5}$ | Transport_Macropinocytosis | .00271 |
| Cell adhesion_Tight junctions | .01317 | Glycolysis and gluconeogenesis p. 2 | .000152 | Transport_RAB3 regulation pathway | .0037 |
| Transcription_P53 signaling pathway | .01426 | Glycolysis and gluconeogenesis p. 2/rodent version | .000167 | Immune response_Antiviral actions of interferons | .00479 |
| Neurophysiologic process_Receptor-mediated axon growth repulsion | .01644 | Glycolysis and gluconeogenesis p. 2/human version | .000281 | Normal wtCFTR traffic/sorting endosome formation | .00612 |
| **Ontology: Top GeneGo process networks** | | Fructose metabolism | .001911 | DNA damage_NHEJ mechanisms of DSBs repair | .00681 |
| Transcription_Transcription by RNA polymerase II | .01626 | Fructose metabolism/rodent version | .00276 | Delta508-CFTR traffic/sorting endosome formation in CF | .00991 |
| Cytoskeleton_Actin filaments | .01972 | Muscle contraction_Delta-type opioid receptor in smooth muscle contraction | .0035 | Immune response_IFN alpha/beta signaling pathway | .01076 |
| Cell adhesion_Synaptic contact | .02144 | Transcription_Role of Akt in hypoxia-induced HIF1 activation | .003772 | Cell adhesion_Endothelial cell contacts by nonjunctional mechanisms | .01076 |
| Reproduction_Spermatogenesis, motility and copulation | .03227 | **Ontology: Top GeneGo process networks** | | **Ontology: Top GeneGo process networks** | |
| Reproduction_Male sex differentiation | .03683 | Muscle contraction | .00024 | Cytoskeleton_Cytoplasmic microtubules | .00013 |
| Cytoskeleton_Spindle microtubules | .1304 | Development_Skeletal muscle development | .00127 | Cell cycle_Mitosis | .00035 |
| Cytoskeleton_Cytoplasmic microtubules | .1371 | Transport_Iron transport | .004586 | Cytoskeleton_Spindle microtubules | .00068 |
| Development_Neuromuscular junction | .1732 | Protein folding_ER and cytoplasm | .009973 | Inflammation_Interferon signaling | .00072 |
| Cell adhesion_Cell junctions | .1881 | Cell adhesion_Cell-matrix interactions | .03411 | Cytoskeleton_Macropinocytosis and its regulation | .00145 |
| Cell adhesion_Attractive and repulsive receptors | .2018 | Cell adhesion_Integrin-mediated cell-matrix adhesion | .03452 | Cell adhesion_Integrin-mediated cell-matrix adhesion | .00498 |
| | | Immune response_Phagocytosis | .03703 | Translation_Translation initiation | .00665 |
| | | Development_Blood vessel morphogenesis | .04052 | Cytoskeleton_Actin filaments | .00762 |
| | | Cell adhesion_Attractive and repulsive receptors | .1177 | Translation_Elongation-Termination | .00786 |
| | | Signal transduction_Insulin signaling | .1177 | Cytoskeleton_Intermediate filaments | .00823 |

Note. Threshold: 1.5 (SILAC ratio), Significance B *P* value <.05, and the sorting method is statistically significant.

optic nerve.[23] This suggests SOD2 as a putative target for future treatment of HSE, in particular to reduce the neurologic sequelae that patients suffer after encephalitis.

We used gene transfer to further investigate the role of SOD2 in human-transformed fibroblasts. Western-blot analysis of healthy cells confirmed the upregulation of SOD2 after poly(I:C) stimulation, and very low levels of SOD2 in UNC-93B$^{-/-}$ cells suggested that the defect affects SOD2 expression (Fig 4, *A*). We detected SOD2 overexpression after transient transfections of pBI-EGFP-MnSOD (SOD2), but not with mock transfected vector (Fig 4, *A*). The measurement of apoptosis in SV40 fibroblasts transfected with SOD2 showed that healthy cells overexpressing SOD2 are protected against apoptosis and that this is also the case for stimulation with poly(I:C). Relative apoptosis measured in poly(I:C)-stimulated UNC-93B$^{-/-}$ cells against their nonstimulated counterpart was higher than similar measurement for healthy controls, indicating UNC-93B$^{-/-}$ patient cells as more susceptible to apoptosis than healthy cells after TLR3 activation. When transfected with SOD2, however, UNC-93B$^{-/-}$ patient cells were protected against apoptosis (Fig 4, *B*). Together, these results suggest that pharmacologic agents that upregulate SOD2 expression or activity could exert a protective antioxidant response mechanism to reduce the cell death associated with TLR3 stimulation in patients with HSE.

## Analysis of a patient with unknown gene defect and without fibroblastic phenotype

Thirty percent of patients with HSE analyzed do not show the fibroblastic phenotype characterized by reduced IFN type I and III production after TLR3 stimulation (data not shown). In these patients, study of the TLR3-stimulated proteome may help delineate the source(s) of the different cellular phenotype. We conducted a SILAC analysis of a patient whose genetic defect is unknown but that produces significant amounts of IFN type I and III after TLR3 stimulation (see Fig E6, *A*, in this article's Online Repository available at www.jacionline.org). The study identified many upregulated proteins shared with stimulated healthy control

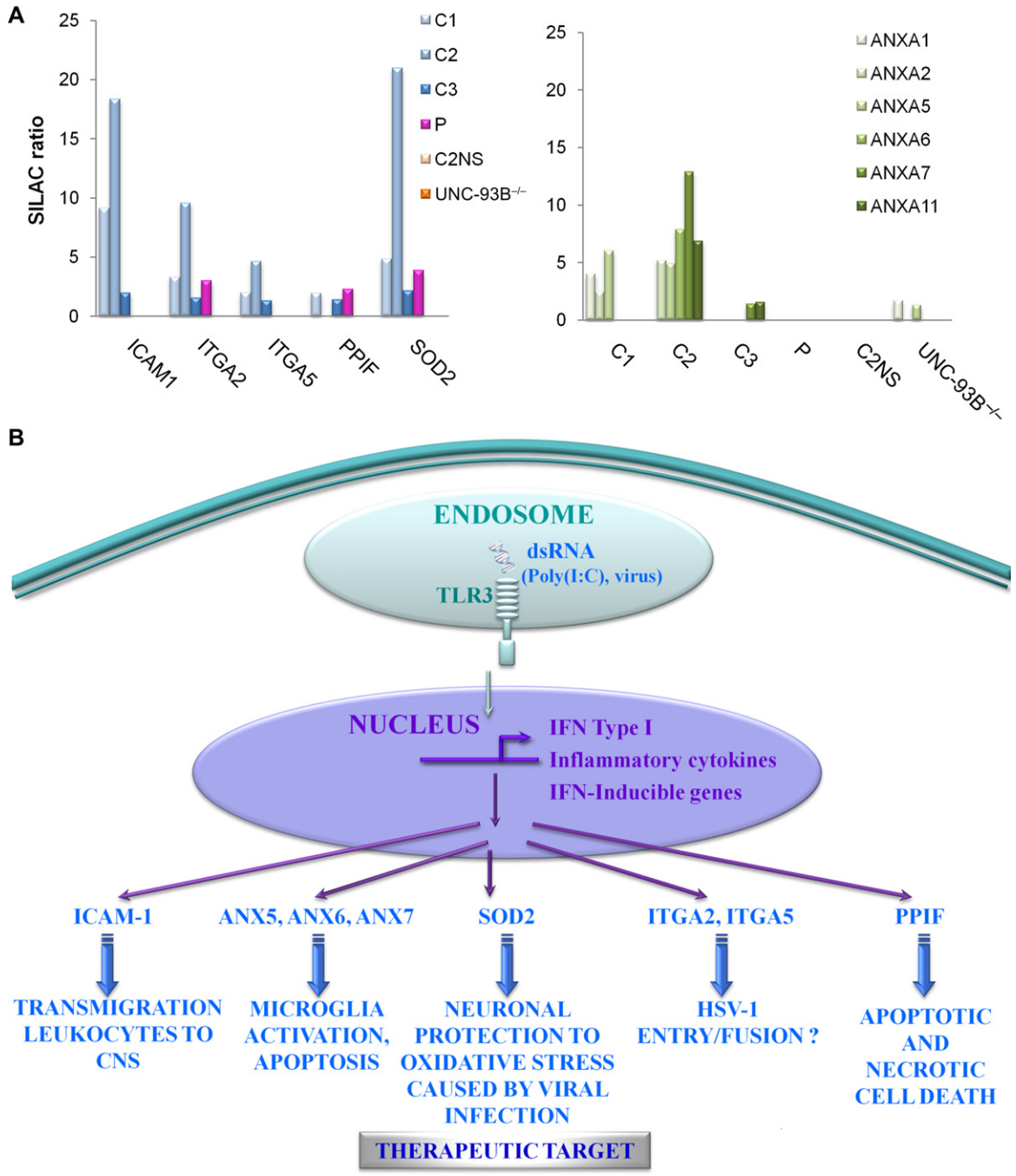


**FIG 3. A,** For proteins with potential biological significance in HSE, the SILAC ratio detected for healthy controls *(C1-3)*, healthy control 2 nonstimulated *(C2NS)*, UNC-93B–deficient patient *(UNC-93B$^{-/-}$)*, and patient with unknown gene defect *(P)*. Significance B *P* value <.05. **B,** Illustration of potential biological significance in immunity against HSE for proteins upregulated after TLR3 activation. *ds*, Double stranded.

samples C1, C2, and C3 that were not observed for UNC93B$^{-/-}$. The proteins shared those highlighted during earlier analysis of the stimulated healthy controls, with the exception of ICAM-1, which was not detected poststimulation (Fig 3, *A*, and Table E6) as confirmed by western-blot analysis (Fig E6, *B*). ITGA5 (H/L = 1.65) and ANX11 (H/L = 1.29) are upregulated in patient sample P, but at a significance ratio just outside the threshold of significance B (<.05) (Table E6). GeneGo analysis also inferred process networks similar to those related to the stimulation of healthy controls, involving immune responses such as IFN signaling and antigen presentation pathways (Table II). This result concurs with previous studies that show cells from patient P to exhibit IFN type I and III production after TLR3 signaling (Fig E6, *A*). Given the extent of overlap between the analysis of TLR3 stimulation effect in patient P and that in healthy control samples, the nondetectable levels of ICAM-1 on TLR3 stimulation in P, identified via proteomic analysis, provide an avenue in this patient for a candidate approach centred on ICAM-1 and related genes/proteins. This would be the first such approach in a patient with HSE to involve pathways beyond TLR3-IFN signaling.

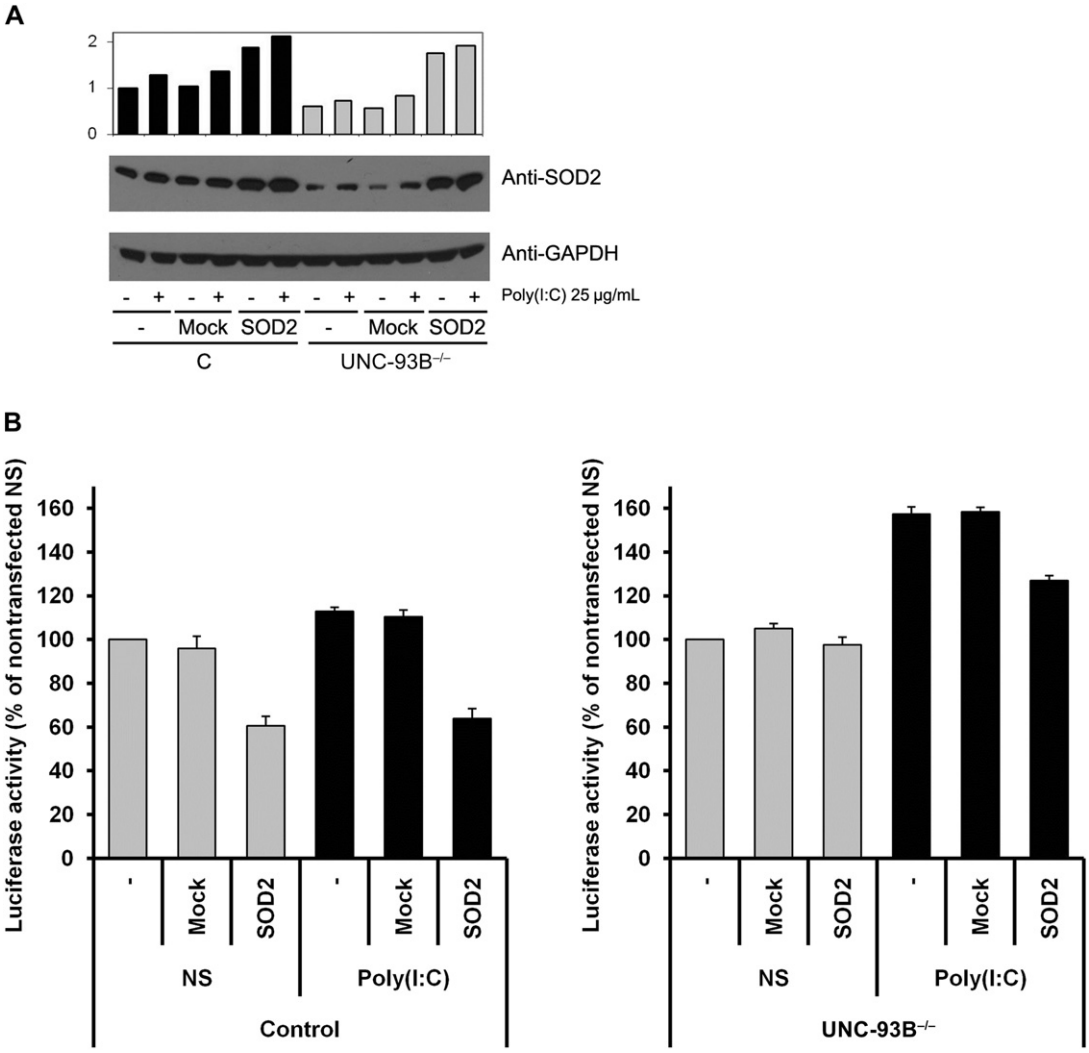


**FIG 4.** Human SV40 fibroblast nontransfected *(−)*, transfected with SOD2 or Mock vector. **A,** Western-blot analysis of SOD2 levels. Densitometry normalized with respect to glyceraldehyde-3-phosphate dehydrogenase, expressed as a fold induction over nonstimulated/nontransfected control cells. The panel is representative of 3 experiments. **B,** Caspase-3/7 activity in nonstimulated *(NS)* or poly(I:C)-stimulated cells. Luciferase activity represented as percentage; 100% is healthy control nonstimulated. Mean values ± SD were calculated from 3 independent experiments. Two-sided test was used, and a *P* value of less than .05 was considered statistically significant. *C*, Healthy control C3; *UNC-93B*$^{-/-}$, UNC-93B–deficient patient; −, nonstimulated; +, poly(I:C) stimulated.

## DISCUSSION

The quantitative SILAC analysis presented here provides important preliminary evidence to suggest that several proteins, pathways, and processes could play important and novel roles in TLR3 response and HSE immunity.

### ICAM-1 upregulation

After TLR3 stimulation, healthy controls C1, C2, and C3 displayed ICAM-1 upregulation, as described previously,[24,25] but there was no corresponding upregulation in UNC-93B$^{-/-}$, patient P, or nonstimulated C2NS (Fig 3, *A*, and Fig E6). ICAM-1 is an intercellular adhesion molecule implicated in HSV-1 infection in the CNS.[26,27] The present results suggest that lack of ICAM upregulation may be an important factor in susceptibility to HSE, especially for those patients (eg, P) who show substantial IFN production and lack the fibroblastic phenotype.

### Upregulation of integrins ITGA2 and ITGA5

We detected ITGA2 and ITGA5 upregulation after TLR3 stimulation in healthy cells but not in C2NS or UNC-93B$^{-/-}$ (Fig 3, *A*). Cells from patient P showed significant upregulation of ITGA2 (Fig 3, *A*) and upregulation of ITGA5 (H/L = 1.65) just beyond the significance threshold used (Table E6). Some studies have demonstrated that integrins are necessary for HSV-1 entry/fusion in cells[28] and ITGA2 is upregulated in chronic hepatitis virus infection.[29] The present results identify specific integrins upregulated following TLR3 activation and whose further investigation might offer new insights into HSE susceptibility.

### Upregulation of annexins

After TLR3 stimulation in healthy cells, we detected upregulation of several annexins (Fig 3, *A*). Microglial cells, after activation in response to harmful stimuli, are able to induce neuronal

cell death by ANX1[30] and ANX5 upregulation.[31] It has been shown that TLR3 activation with poly(I:C) and HSV-1 infection induce apoptosis by enhancing ANX5 levels.[32-34] The present data suggest possible roles for ANX5, ANX6, and ANX7 in the activation and subsequent apoptosis of immune cells in the CNS on viral infection.

## PPIF upregulation

PPIF protein was upregulated after TLR3 stimulation in healthy and patient P cells but not in those with the UNC-93B$^{-/-}$ defect (Fig 3, *A*). PPIF, also called cyclophilin D, is part of the mitochondrial permeability transition pore in the inner mitochondrial membrane. Activation of this pore is thought to be involved in the induction of apoptotic and necrotic cell death. HSV-1 infection of neurons is known to induce cell death, and PPIF has been previously described as a key protein in neuronal cell death.[35-37] This is the first report of a relationship between PPIF and TLR3, suggesting a possible role for PPIF in HSE immunity.

Previous studies have shown that the TLR3 pathway is essential for susceptibility to HSE.[6-8] However, the analysis of many proteins downstream of TLR3 implicated in the TLR3-IFN type I pathway has failed to reveal a genetic defect in most patients analyzed. In 226 patients enrolled in our laboratory, we have detected mutations in *UNC93B1*, *TLR3*, or genes downstream of the TLR3 pathway in a very low percentage. Conversely, study of IFN type I and III production after TLR3 activation in SV40 fibroblasts of patients with HSE has shown that only 30%, of a total of 89 patients analyzed, have normal IFN type I and III production (data not shown). This suggests that despite the importance of the TLR3 pathway in HSE immunity, genetic defect(s) responsible for susceptibility to HSV-1 in the CNS could be due to TLR3-independent pathways, or other TLR3, IFN-dependent pathways that are activated after initial TLR3 activation. Overall, the present results suggest a rich diversity of pathways downstream of TLR3 activation that may be relevant for HSE susceptibility and that invite further investigation.

Proteomic analysis of a patient (P) with unknown gene defect but without the fibroblastic phenotype has revealed a lack of ICAM-1, delineating a cellular phenotype that may assist dissection of this genetic etiology. Finally, an important problem in this pathology is postinfection neurologic sequelae, for which the current treatment is aciclovir, an antiviral drug. However, this treatment is largely uneffective.[2] The present study has now revealed SOD2 as a possible therapeutic target for the prevention of the neurologic sequelae suffered by patients with HSE.

Proteomics has reached the stage where its methods are well developed and capable of generating large, robustly identified, high-resolution quantitative data sets that provide a wealth of knowledge at the systems level. Even for a disease such as HSE, of apparent etiological diversity, coupled with the cellular diversity evident among individuals, proteomics has provided an integrated overview of cellular responses that may be crucial for understanding the dynamics of HSE susceptibility.

We thank the members of the Laboratory of Human Genetics of Infectious Diseases, especially Marjorie Hubeau, Dr C. Guerrera, and Prof L. R. Brown for helpful advice. We thank Mariana Díaz Almiron (Biostatistical Unit, IdiPaz-Hospital La Paz) for the biostatistical analysis. We thank the patient and her family for their participation in this study.

**Clinical implications: Quantitative SILAC-based proteome analysis of TLR3-stimutated human immortalized fibroblasts can delineate cellular phenotypes and may be used to dissect the genetic basis of childhood herpes simplexvirus encephalitis, as well as new potential therapeutics targets.**

## REFERENCES

1. Whitley RJ. Herpes simplex encephalitis: adolescents and adults. Antiviral Res 2006;71:141-8.
2. De Tiege X, Rozenberg F, Heron B. The spectrum of herpes simplex encephalitis in children. Eur J Paediatr Neurol 2008;12:72-81.
3. Abel L, Plancoulaine S, Jouanguy E, Zhang SY, Mahfoufi N, Nicolas N, et al. Age-dependent Mendelian predisposition to herpes simplex virus type 1 encephalitis in Childhood. J Pediatr 2010;157:623-9, 623.e1.
4. Casanova JL, Abel L. Primary immunodeficiencies: a field in its infancy. Science 2007;317:617-9.
5. Alcais A, Abel L, Casanova JL. Human genetics of infectious diseases: between proof of principle and paradigm. J Clin Invest 2009;119:2506-14.
6. Casrouge A, Zhang SY, Eidenschenk C, Jouanguy E, Puel A, Yang K, et al. Herpes simplex virus encephalitis in human UNC-93B deficiency. Science 2006;314:308-12.
7. Zhang SY, Jouanguy E, Ugolini S, Smahi A, Elain G, Romero P, et al. TLR3 deficiency in patients with herpes simplex encephalitis. Science 2007;317:1522-7.
8. Perez de Diego R, Sancho-Shimizu V, Lorenzo L, Puel A, Plancoulaine S, Picard C, et al. Human TRAF3 adaptor molecule deficiency leads to impaired Toll-like receptor 3 response and susceptibility to herpes simplex encephalitis. Immunity 2010;33:400-11.
9. Sancho-Shimizu V, Perez de Diego R, Lorenzo L, Halwani R, Alangari A, Israelsson E, et al. Herpes simplex encephalitis in children with autosomal recessive and dominant TRIF deficiency. J Clin Invest 2011;121:4889-902.
10. Herman M, Ciancanelli M, Ou YH, Lorenzo L, Klaudel-Dreszler M, Pauwels E, et al. Heterozygous TBK1 mutations impair TLR3 immunity and underlie herpes simplex encephalitis of childhood. J Exp Med 2012;209:1567-82.
11. Chapgier A, Wynn RF, Jouanguy E, Filipe-Santos O, Zhang S, Feinberg J, et al. Human complete Stat-1 deficiency is associated with defective type I and II IFN responses in vitro but immunity to some low virulence viruses in vivo. J Immunol 2006;176:5078-83.
12. Shevchenko A, Wilm M, Vorm O, Mann M. Mass spectrometric sequencing of proteins silver-stained polyacrylamide gels. Anal Chem 1996;68:850-8.
13. Ong SE, Blagoev B, Kratchmarova I, Kristensen DB, Steen H, Pandey A, et al. Stable isotope labeling by amino acids in cell culture, SILAC, as a simple and accurate approach to expression proteomics. Mol Cell Proteomics 2002;1:376-86.
14. Ong SE, Foster LJ, Mann M. Mass spectrometric-based approaches in quantitative proteomics. Methods 2003;29:124-30.
15. Mulvey C, Tudzarova S, Crawford M, Williams GH, Stoeber K, Godovac-Zimmermann J. Quantitative proteomics reveals a "poised quiescence" cellular state after triggering the DNA replication origin activation checkpoint. J Proteome Res 2010; 9:5445-60.
16. Cox J, Mann M. MaxQuant enables high peptide identification rates, individualized p.p.b.-range mass accuracies and proteome-wide protein quantification. Nat Biotechnol 2008;26:1367-72.
17. Cox J, Matic I, Hilger M, Nagaraj N, Selbach M, Olsen JV, et al. A practical guide to the MaxQuant computational platform for SILAC-based quantitative proteomics. Nat Protoc 2009;4:698-705.
18. Matsumoto M, Seya T. TLR3: interferon induction by double-stranded RNA including poly(I: C). Adv Drug Deliv Rev 2008;60:805-12.
19. Uematsu S, Akira S. Toll-like receptors and type I interferons. J Biol Chem 2007; 282:15319-23.
20. Rakkola R, Matikainen S, Nyman TA. Proteome analysis of human macrophages reveals the upregulation of manganese-containing superoxide dismutase after toll-like receptor activation. Proteomics 2007;7:378-84.
21. Hill JM, Lukiw WJ, Gebhardt BM, Higaki S, Loutsch JM, Myles ME, et al. Gene expression analyzed by microarrays in HSV-1 latent mouse trigeminal ganglion following heat stress. Virus Genes 2001;23:273-80.
22. Saha RN, Pahan K. Differential regulation of Mn-superoxide dismutase in neurons and astroglia by HIV-1 gp120: implications for HIV-associated dementia. Free Radic Biol Med 2007;42:1866-78.
23. Qi X, Lewin AS, Sun L, Hauswirth WW, Guy J. SOD2 gene transfer protects against optic neuropathy induced by deficiency of complex I. Ann Neurol 2004; 56:182-91.
24. Rydberg C, Mansson A, Uddman R, Riesbeck K, Cardell LO. Toll-like receptor agonists induce inflammation and cell death in a model of head and neck squamous cell carcinomas. Immunology 2009;128:e600-11.

25. Starace D, Galli R, Paone A, De Cesaris P, Filippini A, Ziparo E, et al. Toll-like receptor 3 activation induces antiviral immune responses in mouse sertoli cells. Biol Reprod 2008;79:766-75.
26. Brankin B, Hart MN, Cosby SL, Fabry Z, Allen IV. Adhesion molecule expression and lymphocyte adhesion to cerebral endothelium: effects of measles virus and herpes simplex 1 virus. J Neuroimmunol 1995;56:1-8.
27. Noisakran S, Harle P, Carr DJ. ICAM-1 is required for resistance to herpes simplex virus type 1 but not interferon-alpha1 transgene efficacy. Virology 2001;283:69-77.
28. Parry C, Bell S, Minson T, Browne H. Herpes simplex virus type 1 glycoprotein H binds to alphavbeta3 integrins. J Gen Virol 2005;86:7-10.
29. Bieche I, Asselah T, Laurendeau I, Vidaud D, Degot C, Paradis V, et al. Molecular profiling of early stage liver fibrosis in patients with chronic hepatitis C virus infection. Virology 2005;332:130-44.
30. Parente L, Solito E. Annexin 1: more than an anti-phospholipase protein. Inflamm Res 2004;53:125-32.
31. Li L, Lu J, Tay SS, Moochhala SM, He BP. The function of microglia, either neuroprotection or neurotoxicity, is determined by the equilibrium among factors released from activated microglia in vitro. Brain Res 2007;1159:8-17.
32. Jiang Q, Wei H, Tian Z, Poly I. C enhances cycloheximide-induced apoptosis of tumor cells through TLR3 pathway. BMC Cancer 2008;8:12.
33. Gillis PA, Okagaki LH, Rice SA. Herpes simplex virus type 1 ICP27 induces p38 mitogen-activated protein kinase signaling and apoptosis in HeLa cells. J Virol 2009;83:1767-77.
34. Swarup V, Ghosh J, Duseja R, Ghosh S, Basu A. Japanese encephalitis virus infection decrease endogenous IL-10 production: correlation with microglial activation and neuronal death. Neurosci Lett 2007;420:144-9.
35. Baines CP, Kaiser RA, Purcell NH, Blair NS, Osinska H, Hambleton MA, et al. Loss of cyclophilin D reveals a critical role for mitochondrial permeability transition in cell death. Nature 2005;434:658-62.
36. Li V, Brustovetsky T, Brustovetsky N. Role of cyclophilin D-dependent mitochondrial permeability transition in glutamate-induced calcium deregulation and excitotoxic neuronal death. Exp Neurol 2009;218:171-82.
37. Du H, Guo L, Fang F, Chen D, Sosunov AA, McKhann GM, et al. Cyclophilin D deficiency attenuates mitochondrial and neuronal perturbation and ameliorates learning and memory in Alzheimer's disease. Nat Med 2008;14:1097-105.